Evaluations of Mesogen Orientation in Thin Films of Polyacrylate with Cyanobiphenyl Side Chain

Daisuke Tanaka,[†] *Tasuku Mizuno,*[†] *Mitsuo Hara,*[†] *Shusaku Nagano,*[‡]* *Itsuki Saito,*[§] *Katsuhiro Yamamoto,*[§] *and Takahiro Seki*[†]*

[†] Department of Molecular Design and Engineering, Graduate School of Engineering, Nagoya University, Furo-cho, Chikusa, Nagoya 464-8603, Japan

[‡] Nagoya University Venture Business Laboratory, Nagoya University, Furo-cho, Chikusa, Nagoya 464-8603, Japan

[§] Department of Materials Science and Engineering, Graduate School of Engineering, Nagoya Institute of Technology, Gokiso, Showa, Nagoya 466-8555, Japan

ABSTRACT: The orientation behavior of mesogens in a polyacrylate with cyanobiphenyl (CB) side chain in thin films was investigated in detail by UV-visible absorption spectroscopy and grazing incidence small angle X-ray scattering (GI-SAXS) measurements using both high energy X-ray of Cu *K*α line (λ = 0.154 nm) and low energy synchrotron X-ray (λ = 0.539 nm). By changing the film thickness ranging 7 – 200 nm, it is concluded that the planar orientation is predominant for thin films with thickness below 10 – 15 nm. This planar mesogen orientation

near the substrate surface coexists with the homeotropically aligned CB mesogens in films thicker than 30 nm. For the thinnest 7 nm film, the planar orientation is unexpectedly lost, which is in consort with a disordering of smectic layer structure. Peculiar orienting characteristics of CB mesogen are suggested, which probably stem from the tendency to form an antiparallel arrangement of mesogens due to the strong dipole moment of the terminal cyano group.

1. INTRODUCTION

Understanding the polymer chain behavior in the vicinity of interfaces (substrate and free surfaces) is of practical importance in polymer thin film technologies such as photoresist and coating processes. Therefore, a great deal of fundamental knowledge has been hitherto accumulated. It is widely recognized that various physical properties of polymers in ultrathin film state are deviated from those in the bulk materials. For amorphous polymers, properties of dynamic motions typically reflected to glass transition temperature (T_g)[1–3] and elastic modulus[4] are changed in the thin film state or at the surface.[5–7] For crystalline and semi-crystalline polymers, melting processes,[8] and main chain orientations are of great concern. In the view of material functions, orientation and arrangement of π-conjugated systems near the interfaces play critical roles in carrier transport properties in TFT devices and solar cells.[9,10] Polysilanes possessing σ-conjugated main chains provide the conformational state of backbone simply by UV-visible absorption spectroscopy. Despotopoulou, Frank et al.[11,12] found that the content of all-trans-zigzag conformation (crystalline phase) in poly(*n*-dihexylsilane) (PDHS) film is reduced with decreasing the film thickness. No all-trans-zigzag conformation is observed when the film thickness becomes below approximately10 nm. Nagano and Seki[13,14] prepared built-up

Langmuir-Blodgett (LB) films consisting of PDHS via co-spreading with 4'-pentyl-cyanobiphenyl (5CB) on water. Stepwise depositions of the monolayered PDMS demonstrated that the helical gauche conformation near the substrate abruptly changes to the all-trans-zigzag one at a specific deposition number corresponding to the same thickness.[14]

Compared with the vast amount of studies for amorphous and crystalline (LC) polymers, studies on the anomaly in structure and orientation of side chain liquid crystalline polymers in ultrathin film states is rather unexplored. However, some significant data have been reported.[15–20] Henn et al.[15] discussed the orientational change in mesogens of a smectic polymer at a ultrathin film state by X-ray reflectometry measurements. They observed that the homeotropically aligned rod mesogens becomes planar for films below 10 nm when the film is in the smectic C* phase. Mensinger et al.[16] pointed out that a surface-induced parallel ordering of smectic layer is affected to ca. 50 nm distance from the substrate surface. Elben and Strobl[17] found a smectic layer structuring at the surface for some side chain liquid crystalline polymers even far above the isotropization temperature (T_i). Van der Wielen et al.[18,19] indicated the existence of adhered layer below 1 nm thickness with the mesogen anchored parallel with the substrate, which leads to autophobic dewetting properties. More recently, Morikawa et al.[21] reported a thinning effect for a cylinder-forming LC block copolymer. In this case with the mesoscopic structure, a homeotropic to planar orientation change occurs at approximately 60 nm thickness.

<Scheme 1>

In general, the rodlike mesogens tend to orient vertically with the free surface as confirmed by both theoretical simulations[22–24] and experimental results.[25,26] Accordingly, the side chain LC polymers are mostly aligned homeotropically.[27–30] The significant influence of the free surface is

obvious from the fact that the mesogen orientation is changed to a planar orientation when the free surface is covered by another layer or material.[29,31–33] However, we recently found that a cyanobiphenyl (CB)-containing polymethacrylate (PCBMA) exceptionally exhibits the planar orientation regardless of the fact that the homologous polyacrylate (PCBA, Scheme 1) orients homeotropically.[33] This unexpected orientating behavior should be responsible for the difference in the main chain rigidity, however a rational explanation is not given. In this former work, grazing incidence angle X-ray scattering (GI-SAXS) measurements indicated that, unlike other side chain LC polymers, a considerable amount of planarly oriented mesogens are stubbornly retained within the PCBA film although most of mesogens adopt the homeotropic orientation. The existence of significant amount of planarly oriented mesogens in PCBA seems to provide a clue to understand the perplexing mesogen orientation behaviour of PCBMA.

In the above contexts, we have further proceeded with an investigation to elucidate in detail the orientation behavior of PCBA films by UV-visible spectroscopic and GI-SAXS measurements by systematically changing the film thickness. In addition to the laboratory GI-SAXS with high energy X-ray (λ = 0.154 nm, (8.05 keV, hard X-ray)), we newly carried out the GI-SAXS measurements using a low energy synchrotron X-ray beam (λ = 0.539 nm (2.30 keV, tender X-ray)) with precisely varied incident angles to the film sample.[34] With the tender X-ray, the depth-resolved information is expected to be obtained because the penetration length is at the comparable level of the film thickness. By means of these evaluations, it is proposed here that CB mesogens orient in the in-plane direction near the substrate surface in a region below 10 – 15 nm. It is also found here that an extremely thin state as 7 nm, such planar orientation is lost in consort with a vanishing of smectic layer structuring. We infer that such orientating manners are

characteristic for the polymers with side chains possessing a mesogen with a strongly polar cyano group at the terminal.

2. EXPERIMENTAL SECTION

2.1 Materials

The synthesis of polymer (PCBA), their characterizations were described previously. The molecular mass data of PCBA and thermophysical properties of the resulting polymers were as follows. PCBA: $M_n = 1.2 \times 10^4$ (n = 28), $M_w/M_n = 1.83$, and glass–13 °C–smectic A–95 °C–isotropic (Figures S1 and S2). T_i reasonably agreed with that reported previously for a corresponding polymer with $(CH_2)_{11}$ spacer (87 °C).[35] The layer spacing of the smectic A of both LC polymers in the bulk state were evaluated by X-ray scattering measurements using a FR-E X-ray diffractometer equipped with a R-AXIS IV two-dimensional (2D) detector (Rigaku Co.). The layer spacings (d) of smectic A layer of PCBA was estimated to be 4.6 nm ($2\theta = 1.9°$).

2.2 Measurements

UV-visible absorption spectra were taken on an Agilent 8453 spectrometer. Temperature of the film sample was controlled by using a custom-made hot stage for microscope (Imoto Machinery Co. Ltd.)

GI-SAXS measurements using a hard X-ray were performed with a FR-E X-ray diffractometer equipped with R-AXIS IV two-dimensional (2D) detector (Rigaku Co.) at a voltage of 45 kV, current of 45 mA, and irradiation time of 2 h to create copper Cu K_a radiation (λ = 0.154 nm).

Camera length was 300 mm. X-ray scattering patterns were recorded on an imaging plate (Fujifilm Co.). Temperature of the film sample was controlled using a ceramic heating system.

GI-SAXS measurements by using low energy X-ray were performed at BL-15A2 at the Photon Factory, KEK, Tsukuba in Japan. Experimental details of the GI-SAXS measurements were previously described.[36] The BL-15A2 is an undulator beamline that offers X-rays in wide energy range from 2.1 to 15 keV (energy resolution: 2 x 10^{-4}). In our measurements, the X-ray energy was set at 2.30 keV (0.539 nm) and the sample-to-detector distance was 830 ± 5 mm. The X-ray incident angles were valuable between 0.290° and 0.620°, and PILATUS 2M designed for usage in vacuum was used as a detector for the 2D scattering pattern. X-ray exposure time of 300 s was sufficient to obtain a clear scattering pattern. The critical angle (α_c) for the film samples was obtained from the Yoneda line in the GI-SAXS pattern observed with hard X-rays (λ = 0.1 nm) at BL03XU in SPring-8, Harima, Japan, with the simple calculation of the mass density of the PCBA.(5) The α_c of the PCBA film was calculated as 0.54° at 2.30 keV.

The contact angle of a water droplet was estimated with a FACE CA-XP contact angle meter (Kyowa Interface Science). The averaged values of five measurements were obtained.

2.3 Procedures

Polymer films on quartz plates were prepared by spin casting from 0.12 – 3.0 % (by weight) chloroform solutions. Spincast films were prepared with a Kyowariken K-359S1 spincoater at 2000 rpm. The spincast film samples were annealed at 135 °C, cooled to a target temperature, kept for 10 min, and then subjected to the measurements. Film thickness was estimated by using a white light interferometric microscope (BW-S501, Nikon Instruments). After scratching the film with a spatula, height difference between the film and substrate surfaces was estimated. A

good correlation was obtained between the concentration the chloroform solution for spincasting and the resultant film thickness (data not shown).

Quartz plates (1.5 × 1.5 cm) were washed with saturated potassium hydroxide ethanol solution, followed by washing with pure water under sonication. The static contact angle of water was 8 ± 2°. Thus, the surface of quartz plates was hydrophilic.

<Figure 1>

3. RESULTS AND DISCUSSION

3.1 Morphologies of the film

Figure 1 shows surface film morphologies and height profiles obtained by white light interference microscopy for films with 140, 30, and 7 nm thickness. These films were annealed at 135 °C and cooled down to room temperature. The vertical artificial line in each image is a scratched area with a spatula. As indicated, the film surfaces were reasonably flat, and undulations and dewetting due to film instability after annealing were not observed even for the thinnest 7 nm film. Therefore, the flatness of films is guaranteed for the interpretations of the mesogen orientation.

<Figure 2>

3.2 UV-visible absorption spectroscopy

UV-visible absorption spectra were taken for PCBA films changing the thickness from 200 nm to 7 nm. Among them, data of four representative thicknesses of 140 (a), 30 (b), 15 (c), and 7 nm (d) are indicated in Figure 2. These films were first annealed at 135 °C (isotropic in the bulk) and

then cooled down to 80 °C (smectic A in the bulk). Two absorption bands were observed at 300 nm and 225 nm. The absorption band at 225 nm is insensitive to the mesogen orientation, and the transition moment of the π–π* band at 300 nm is parallel with the long axis of the CB mesogen.[37] To provide a sufficiently randomized state, heating up to considerably higher temperatures above T_i (95 °C) was required. In this series of experiments, 135 °C was selected to fulfill the sufficiently randomized condition. Below this temperature, the UV-visible spectral shape was continuously enhanced with increasing temperature (Figure S3). The reduction in absorbance at 300 nm at 80 °C compared with that at 135 °C reflects a reorientation to a more vertical orientational state in the smectic A phase. For films from 140 to 15 nm thickness, the extent of this reduction became smaller, showing that CB mesogens became more planarly oriented along with thinning of the films. Unexpectedly, for the 7 nm thick film, the extent of reduction became larger again.

<Figure 3>

Figure 3a displays absorbance at 135 °C and 80 °C as a function of film thickness for all films examined. Original spectral data are shown in Figure S4. These absorbance values were almost proportional with the film thickness (Note that the axis of film thickness is changed between 60 and 150 nm).

The absorbance ratio of A_{300}/A_{225} can be a measure of CB orientation in the zenithal (out-of-plane) direction. In Figure 3b, A_{300}/A_{225} was plotted against film thickness. Except for the 7 nm thick film, all A_{300}/A_{225} values at 135 °C were essentially unchanged ranging 1.08 – 1.21. This value for 7 nm thick film was significantly deviated to a lower value of 0.8.

At 80 °C, A_{300}/A_{225} values in the thicker regions (above 60 nm) were essentially identical ranging 0.45 – 0.50, showing that CB mesogens adopt a homeotropic orientation in the same manner. However, in the thinner region below 30 nm, it significantly increased and reached 0.93 at 10 nm thickness, and this value suddenly decreased to 0.50 at 7 nm thickness. We carefully checked the data for the 7 nm film, and confirmed that this irregular value was highly reproducible. As stated in section 3.1, this unexpected deviation is not originated form a morphological change of the film. This exceptional behavior observed for the 7 nm thick film will be discussed later.

Change in the surface energy of substrates should alter the surface alignment property of LC materials,[38] and thus an exploration with other substrate surfaces would be of value. Essentially the same results were obtained for quartz plates before and after the cleaning procedure, static contact angle of water being 66 ± 1° and 8 ± 2°, respectively. Unfortunately, when more hydrophobic quartz substrates modified with 1,1,1,3,3,3-hexamethyldisilazane were used, dewetting of PBCA films readily occurred, and proper comparisons could not be made. We assume that the mesogen orientation behavior on a planar solid surface is unchanged as far as the stable films are formed.

<Figure 4>

3.3 GI-SAXS measurements with Cu *K*α X-ray (Hard X-ray)

Figures 4a-c indicates GI-SAXS data taken with hard X-ray (λ = 0.154 nm) using a Cu *K*α line for 140 nm (a), 30 nm (b), and 15 nm (c) thick at 80 °C. In each part, 2D image and 1D profile are displayed in the upper and lower figures. In Figure S5, GI-SAXS data including other thicknesses are summarized. For 140 nm thick film, the scattering peaks corresponding to *d*

(layer spacing) = 4.6 nm (100) and 2.3 nm (200) were clearly observed in both out-of-plane and in-plane directions (a). The peaks in the out-of-plane direction became very small in 30 nm thick film, and essentially no peaks were observed for 15 nm thick film, although those in the in-plane direction were clearly observed. 1D profiles displaying both intensity profiles in the out-of-plane (red line) and in-plane (black line) directions indicate well the above situations. These results unequivocally indicates that the planarly and homeotropically oriented CB mesogens are coexisting in the films with thickness greater than 30 nm, and CB mesogens were oriented only planarly at 15 nm thickness.

It is to be noted that the scattering spots were observed selectively in the azimuthal and zenithal directions, and essentially no scattering signals were observed in other intermediate directions. This indicates that the mesogens are aligned essentially only in the planar or homotropic state in the films, and orientational change should occur suddenly at a critical distance from the surface with negligible gradual transition region.

Figure 4d shows data for the 140 nm film at 90 °C, slightly below T_i (95 °C). In comparison with the data at 80 °C (a), approaching to T_i of the bulk leads to a large reduction of the out-of-plane signals, indicative of the loss of orientational order of the homeotropically aligned CB mesogens. Nevertheless, the peaks in the in-plane direction were hardly affected at this temperature. This fact strongly suggests that the planarly anchored CB mesogens are firmly fixed near the substrate surface.

For the 7 nm thick film, no appreciable scattering signals were obtained (Figure S5f), which indicates that the smectic layer is no longer formed in this thinnest film. This can be correlated to the anomaly in the spectroscopic measurements in section 3.2.

<Figure 5>

3.4 GI-SAXS measurements with low energy X-ray (tender X-ray)

The penetration depth (Λ) is defined as the length attenuated to 1/e of intensity by X-ray from surface. The Λ value is strongly dependent upon X-ray energy and incident angle (α_i).[36] In the above GI-SAXS measurements with the hard X-ray of Cu $K\alpha$, the X-ray penetration depth steeply increases with α_i and reaches over 1000 nm at the critical angle of total reflection (α_c). Thus, previous GI-SAXS data with Cu $K\alpha$ provide information on the structure of overall thickness. On the other hand, the penetration of the lower energy (tender) X-ray gradually penetrates from the film surface with increase of α_i (Figure S6). The GI-SAXS measurements with the lower energy X-ray provide depth-resolved structural information.

In this context, GI-SAXS measurements with a synchrotron X-ray (λ = 0.539 nm, 2.30 keV) were achieved at various α_i. Figure 5 shows the 2D scattering images (q_y–q_z plane) for 30 nm thick film at room temperature. As mentioned above, CB mesogens at this thickness are oriented both in the homeotropic and planar directions in a comparable amount. The α_c in this sample was estimated at ca. 0.54 ° for this X-ray energy. Under conditions of $\alpha_i < \alpha_c$, scattering signals in thin film observed only the out-of-plane direction (Figure 5a–c). Λ is estimated as the range less than 10 – 20 nm in these conditions (see Figure S6). These results clearly indicate that the CB mesogens are oriented homeotropically in the free surface region. Under the larger α_i conditions ($\alpha_i > \alpha_c$), the out-of-plane scatterings were split into two peaks in the q_z axis direction (Figure 5d–f). The split peaks originate from the transmitted X-ray through the film and then reflected on the substrate, and directly reflected one at the film surface.[36] Therefore, the higher q_z peak of the split peaks can be assigned to the scattering from the reflection path on the film

surface. The split spots indicate that the X-ray beam actually penetrated through the overall film thickness and reached the substrate interface. Under conditions of $\alpha_i > \alpha_c$ ($\Lambda > 100$ nm), the peaks in the in-plane direction due to the planar orientation were clearly observed as indicated by arrows in Figure 6d–f. These azimuthal signals undoubtedly originate from the mesogens near the substrate surface.

The same sets of measurements were conducted for a thicker film of 140 nm. In this case, no trace of the peaks in the in-plane direction was observed even under $\alpha_i > \alpha_c$ conditions (Figure S7). Due to the decrease in penetrative power of low energy X-ray propagation, the in-plane scatterings from the bottom of the film would be absorbed inside the film and faded away through the relatively long optical path. In addition, the out-of-plane scatterings were observed as the azimuthally arc signals. The surface roughness of the film should be slightly increased by the shrinkage during the cooling from the isotropic state to the LC state (root-mean-square roughness = 1.5–1.7 nm).

<Table 1>

3.5 Contact angle measurements

To obtain information on the free surface side, contact angle measurements for water droplet were conducted. Static contact angles of water droplet (θ_w) on PCBA films on varied film thickness were evaluated. The films were annealed at 135 °C and then slowly cooled down to room temperature. As shown in Table 1, θ_w values were almost constant at all thickness, and no significant correlation between θ_w and the mesogen orientation was admitted. This fact show that the chemical composition of the uppermost surface is not substantially affected by the difference

in the mesogen orientation, or the mesogen in this surface region is reoriented by the contact with water.

<Figure 6>

3.6 Mesogen orientation model

Based on the overall data of UV-visible absorption spectroscopic and X-ray measurements using hard and tender X-rays, the orientation models of CB mesogens in PCBA thin films at various thickness are shown schematically in Figure 6. In thicker films as 140 nm (a), most of CB mesogens are aligned homeotropically. However, a substantial amount of planarly anchored CB mesogens exist near the substrate surface as shown by the hard X-ray GI-SAXS measurements (Figure 4). At 30 nm thickness (b), the amounts of homeotropically and planarly aligned CB mesogens become comparable, where depth-resolved information can be obtained by the tender X-ray GI-SAXS measurements changing α_i (Figure 5). In the films of 10 – 15 nm thickness, most of the CB mesogens are aligned planarly. When the film becomes even thinner from this critical level as 7 nm, the planar alignment near the surface is lost in consort with the loss of liquid crystal structuring (antiparallel packing of mesogens). Further interpretations for these phenomena are given in the following section.

3.7 On the peculiarity of cyano-terminated mesogen

We have investigated orientation behavior of various kinds of side chain LC polymers, including azobenzene[27,28] and phenyl benzoate[29] as mesogens, and polymethacrylate[27,29] and a backbone formed via ring opening metathesis polymerization[28] as main chains. Spincast films of all these polymers commonly exhibit the homoetropic orientation without discernable in-plane scattering

signals in the hard X-ray GI-SAXS. These facts indicate that the existence of planarly oriented mesogen near the surface is negligible for other side chain polymers. Therefore, the mesogen orientation behavior of CB is unusual. We assume that this peculiarity originates from the antiparallel cooperative interaction between the CB mesogens[39] through the strong dipole (4.05 Debye)[40] interaction. Peculiarities of CB mesogens for the aggregation structure have also been found in the assembly process of low-molecular-mass[40] LCs and relaxation behavior in polymer LCs.[41] Presumably, the existence of firmly remaining planar mesogens is related to the stabilized antiparallel bilayer formation. Planarly anchored (adsorbed) mesogens in contact with the substrate surface can induce the parallel orientation of a considerable amount of neighboring CB mesogens through the strong cooperativity. If the mesogens were aligned in a planar way to 10 – 15 nm away from the surface, approximately 20 to 30 mesogens are stacked with the planar orientation (The face to face mesogen distance should be ca. 0.45 nm[42]).

In the thinnest case of 7 nm thick film, no smectic layer formatin is admitted in both in-plane and out-of-plane directions. At this thinnest level, the liquid crystallinity would be lost, and therefore the cooperativity among the side chains no longer works. Thus, rational comparisons with films above and below the critical thickness (approximately 10 nm) cannot be made.

It is to be noted that the PCBA films need to be heated up to 135 °C, a temperature 40 °C higher than T_i (95 °C), to allow a full orientational randomization of CB chromophores. These results can be compared with X-ray reflectivity data reported by Elben and Strobl.[17] They demonstrated that smectic layers exist at the boundary regions (presumably at the substrate surface) at considerably higher temperatures from T_i in the bulk state. Among four side chain LC polymer samples explored, this effect is distinguished for a polymer with a mesogen with a terminal cyano group. The boundary smectic layers are still observed at a temperature even

60 °C higher than T_i of the bulk sample. Our data reasonably support their results. To discuss the isotropic state in the thin film state of LC polymers, particular care should be taken. Also in this respect, the peculiar nature of the cyano containing mesogen is stressed.

We have reported that the polymethacrylate homologue of PCBA (PCBMA) exceptionally adopts the persistent planar orientation even for thicker films.[33] This can be regarded as the extreme situation observed for planarly orienting system of PCBA. The orientation of homeotropic or planar mode is supposedly governed by a balance between the homeotropic anchoring of rodlike molecules at the free surface resulting from the size exclusion effect[43] and the planar anchoring at the substrate surface.[44] The hindered rotation in the backbone of PCBMA should impede the motion of CB side chain to a large extent,[45,46] and the antiparallel packing structure may not be readily broken even at the free surface. Thereby, the planar orientation will be retained regardless of the film thickness. Experimentally, surface-selective detections of cyano groups by sum frequency generation spectroscopy will be helpful to obtain the information on the mesogen orientation on the topmost surface. This approach should be involved in the future investigations.

4. CONCLUSION

In the view of practical applications, side chain LC polymers are widely studied for optical functional materials such as holographic optical recording and information modulation devices. To obtain sufficient optical effects, relatively thick films typically at micrometer levels are used. Probably for this reason, sufficient attentions have not been paid for LC polymers in the ultrathin film state. Together with our previous report,[33] series of our explorations revealed the

characteristic features of CB-side chain LC polymers. Interestingly, they are routinely investigated LC polymers for various purposes, yet the peculiarities in the thin film state have not been noticed to date. The present data have shown the existence of planarly anchored CB mesogens with 10 – 15 nm thickness near the substrate surface. We insist here that this planar orientation is not attained via the ultrathinning effect, but intrinsically exists neat the substrate also for the thicker films. CB and other cyano-containing other mesogens tend to form antiparallel mesogen arrangement, and this structuring feature leads to peculiarities as also have been pointed out in other systems.[17,40,41] When the film becomes thinner than the critical level (7 nm thick), the layer structuring is lost, which impedes the LC cooperativity to vanish the planar alignment at the substrate surface. It is emphasized that further accumulation of fundamental and precise knowledge on the ultrathin state of LC polymers is required for the development of LC film technologies.

ASSOCIATED CONTENT

Supporting Information.

The Supporting Information is available free of charge on the ACS Publications website at DOI: …..

Synthesis of PCBA, DSC, UV-visible absorption spectra, detailed GI-SAXS data (hard X-ray), penetration depth profile of X-ray, and GI-SAXS (tender X-ray) for 140 nm film (PDF).

AUTHOR INFORMATION

Corresponding Author

*E-mail: snagano@apchem.nagoya-u.ac.jp

*tseki@apchem.nagoya-u.ac.jp

Author Contributions

The manuscript was written through contributions of all authors. All authors have given approval to the final version of the manuscript. The manuscript was written through contributions of all authors.

ACKNOWLEDGMENT

This work was supported by a Grant-in-Aid for Scientific Research (S23225003 to TS and B25286025 to SN), and for Young Scientists (B25810117 to MH) from The Ministry of Education, Culture, Sports, Science and Technology (MEXT), Japan. This work was in part supported in part by a Grant-in-Aid for Scientific Research on Innovative Areas "Photosynergetics" (No. 15H01084) from MEXT, Japan. Soft X-ray GI-SAXS measurements were performed at the Photon Factory of High Energy Accelerator Research Organization (approval 2014G169 to KY).

REFERENCES

(1) Forrest, J. A.; Dalnoki-Veress, K. The glass transition in thin polymer films. *Adv. Colloid Interface Sci.* **2001**, *94*, 167-195.

(2) Keddie, J. L.; Jones, R. A. L.; Cory, R. A. Size-Dependent Depression of the Glass Transition Temperature in Polymer Films. *Eur. Phys. Lett.* **1994**, *27*, 59-64.

(3) Prucker, O.; Christian, S.; Bock, H.; Rühe, J.; Frank, C. W.; Knoll, W. On the glass transition in ultrathin polymer films of different molecular architecture. *Macromol. Chem. Phys.* **1998**, *199*, 1435-1444.

(4) Torres, J. M.; Stafford, C. M.; Vogt, B. D. Elastic Modulus of Amorphous Polymer Thin Films: Relationship to the Glass Transition Temperature. *ACS Nano*. **2009**, *3*, 2677-2685.

(5) Tanaka, K.; Takahara, A.; Kajiyama, T. Rheological Analysis of Surface Relaxation Process of Monodisperse Polystyrene Films. *Macromolecules* **2000**, *33*, 7588-7593.
(6) Tanaka, K.; Hashimoto, K.; Kajiyama, T.; Takahara, A. Visualization of Active Surface Molecular Motion in Polystyrene Film by Scanning Viscoelasticity Microscopy. *Langmuir* **2003**, *19*, 6573-6575.
(7) Ediger, M. D.; Forrest, J. A. Dynamics near Free Surfaces and the Glass Transition in Thin Polymer Films: A View to the Future. *Macromolecules* **2013**, *47*, 471-478.
(8) Kim, J. H.; Jang, J.; Zin, W-C. Thickness Dependence of the Melting Temperature of Thin Polymer Films. *Macromol. Rapid Commun.* **2001**, *22*, 386-389.
(9) Tumbleston, J. R.; Collins, B. A.; Yang, L.; Stuart, A. C.; Gann, E.; Ma, W.; You, W.; Ade H. The influence of molecular orientation on organic bulk heterojunction solar cells. *Nat. Photon.* **2014**, *8*, 385-391.
(10) Vohra, V.; Kawashima, K.; Kakara, T.; Koganezawa, T.; Osaka, I.; Takimiya, K.; Murata, H. Efficient inverted polymer solar cells employing favourable molecular orientation. *Nat. Photon.* **2015**, *9*, 403-408.
(11) Despotopoulou, M. M.; Frank, C. W.; Miller, R. D.; Rabolt, J. F. Role of the Restricted Geometry on the Morphology of Ultrathin Poly(di-n-hexylsilane) Films. *Macromolecules* **1995**, *28*, 6687-6688.
12. Frank, C. W.; Rao, V.; Despotopoulou, M. M.; Pease, R. F. W.; Hinsberg, W. D.; Miller, R. D.; Rabolt, J. F. Structure in Thin and Ultrathin Spin-Cast Polymer Films. *Science* **1996**, *273*, 912-915.
(13) Nagano, S.; Seki, T.; Ichimura, K. Monolayer Formation of Hydrophobic Polysilane on Water through Hybridization with Liquid Crystal Molecules. *Langmuir* **2001**, *17*, 2199-2205.
(14) Nagano, S.; Seki, T. Abrupt Interfacial Transitions of Hydrophobic Polysilanes As Probed via Liquid Crystal-Assisted Stepwise Deposition. *J. Am. Chem. Soc.* **2002**, *124*, 2074-2075.
(15) Henn, G.; Stamm, M.; Poths, H.; Rücker, M.; Rabe, J. P. Influence of order in thin smectic polymer films on the structure at the surface. *Physica B* **1996**, *221*, 174-184.
(16) Mensinger, H.; Stamm, M.; Boeffel, C. Order in thin films of a liquid crystalline polymer. *J. Chem. Phys.* **1992**, *96*, 3183-3190.
(17) Elben, H.; Strobl, G. Smectic surface structures in the isotropic phase of liquid-crystalline polymers studied by x-ray reflectivity. *Macromolecules* **1993**, *26*, 1013-1018.
(18) van der Wielen, M. W. J.; Cohen Stuart, M. A.; Fleer, G. J.; de Boer, D. K. G.; Leenaers, A. J. G.; Nieuwhof, R. P.; Marcelis, A. T. M.; Sudhölter, E. J. R. Order in Thin Films of Side-Chain Liquid-Crystalline Polymers. *Langmuir* **1997**, *13*, 4762-4766.
(19) van der Wielen, M. W. J.; Cohen Stuart, M. A.; Fleer, G. J. Autophobicity and Layering Behavior of Thin Liquid-Crystalline Polymer Films. *Langmuir* **1998**, *14*, 7065-7071.
(20) Wu, J-S.; Fasolka, M. J.; Hammond, P. T. Mixed Surface Morphologies of Well-Defined Smectic Diblock Copolymer Ultrathin Films. *Macromolecules* **2000**, *33*, 1108-1110.
(21) Morikawa, Y.; Nagano, S.; Watanabe, K.; Kamata, K.; Iyoda, T.; Seki, T. Optical Alignment and Patterning of Nanoscale Microdomains in a Block Copolymer Thin Film. *Adv. Mater.* **2006**, *18*, 883-886.
(22) Scaramuzza, N.; Berlic, C.; Barna, E. S.; Strangi, G.; Barna, V.; Ionescu, A. T. Molecular Simulation of the Free Surface Order in NLC Samples. *J. Phys. Chem. B* **2004**, *108*, 3207-3210.

(23) Chen, S-M.; Hsieh, T-C.; Pan, R-P. Magnetic-field-induced Fréedericksz transition and the dynamic response of nematic liquid-crystal films with a free surface. *Phys. Rev. A* **1991**, *43*, 2848-2857.
(24) Canabarro, A. A.; de Oliveira, I. N.; Lyra, M. L. Homeotropic surface anchoring and the layer-thinning transition in free-standing films. *Phys. Rev. E* **2008**, *77*, 011704.
(25) Ocko, B. M.; Braslau, A.; Pershan, P. S.; Als-Nielsen, J.; Deutsch, M. Quantized layer growth at liquid-crystal surfaces. *Phys. Rev. Lett.* **1986**, *57*, 94-97.
(26) Pershan, P. S. Structure of surfaces and interfaces as studied using synchrotron radiation. Liquid surfaces. *Faraday Discuss. Chem. Soc.* **1990**, *89*, 231-245.
(27) Uekusa, T.; Nagano, S.; Seki, T. Highly Ordered In-Plane Photoalignment Attained by the Brush Architecture of Liquid Crystalline Azobenzene Polymer. *Macromolecules* **2009**, *42*, 312-318.
(28) Haque, H. A.; Kakehi, S.; Hara, M.; Nagano, S.; Seki, T. High-Density Liquid-Crystalline Azobenzene Polymer Brush Attained by Surface-Initiated Ring-Opening Metathesis Polymerization. *Langmuir* **2013**, *29*, 7571-7575.
(29) Fukuhara, K.; Nagano, S.; Hara, M.; Seki, T. Free-surface molecular command systems for photoalignment of liquid crystalline materials. *Nat. Commun.* **2014**, *5*, 3320.
(30) Asaoka, S.; Uekusa, T.; Tokimori, H.; Komura, M.; Iyoda, T.; Yamada, T.; Yoshida, H. Normally Oriented Cylindrical Nanostructures in Amphiphilic PEO–LC Diblock Copolymers Films. *Macromolecules* **2011**, *44*, 7645-7658.
(31) Fukuhara, K.; Fujii, Y.; Nagashima, Y.; Hara, M.; Nagano, S.; Seki, T. Liquid-Crystalline Polymer and Block Copolymer Domain Alignment Controlled by Free-Surface Segregation. *Angew. Chem. Int. Ed.* **2013**, *52*, 5988-5991.
(32) Komura, M.; Yoshitake, A.; Komiyama, H.; Iyoda, T. Control of Air-Interface-Induced Perpendicular Nanocylinder Orientation in Liquid Crystal Block Copolymer Films by a Surface-Covering Method. *Macromolecules* **2015**, *48*, 672-678.
(33) Tanaka, D.; Nagashima, Y.; Hara, M.; Nagano, S.; Seki, T. Alternation of Side-Chain Mesogen Orientation Caused by the Backbone Structure in Liquid-Crystalline Polymer Thin Films. *Langmuir* **2015**, *31*, 11379-11383.
(34) Saito, I.; Miyazaki, T.; Yamamoto, K. Depth-Resolved Structure Analysis of Cylindrical Microdomain in Block Copolymer Thin Film by Grazing-Incidence Small-Angle X-ray Scattering Utilizing Low-Energy X-rays. *Macromolecules* **2015**, *48*, 8190-8196.
(35) Ikeda, T.; Kurihara, S.; Karanjit, D. B.; Tazuke, S. Photochemically induced isothermal phase transition in polymer liquid crystals with mesogenic cyanobiphenyl side chains. *Macromolecules* **1990**, *23*, 3938-3943.
(36) Lee, B.; Park, I.; Yoon, J.; Park, S.; Kim, J.; Kim, K-W.; Chang, T.; Ree, M. Structural Analysis of Block Copolymer Thin Films with Grazing Incidence Small-Angle X-ray Scattering. *Macromolecules* **2005**, *38*, 4311-4323.
(37) Taguchi, D.; Manaka, T.; Iwamoto, M. In situ Observations of Orientational Ordering Process of 4'- n -pentyl-4-cyanobiphenyl Ultra-Thin Film Using Polarized Absorption Measurements. *Jpn. J. Appl. Phys.* **2005**, *44*. 1037-1040.
(38) Cognard, J. Alinment of Nematic Liquid Crystals and Their Mixtures. *Mol. Cryst. Liq. Cryst.* **1982**, *Suppl 1*, 1-77.
(39) Collings, P. J.; Hird, M. Calamitic liquid crystals-nematic and smectic mesophases. *Introduction to Liquid Crystals: Chemitry and Physics*; Taylor & Francis, London, 1997.

(40) Lansac, Y.; Glaser, M. A.; Clark, N. A. Microscopic structure and dynamics of a partial bilayer smectic liquid crystal. *Phys. Rev. E* **2001**, *64*, 051703.
(41) Salehli, F.; Yildiz, S.; Ozbek, H.; Uykur, E.; Gursel, Y. H.; Durmaz, Y. Y. Peculiarities of δ- and α-relaxations in thermotropic side chain liquid crystalline polymers with and without nematic reentrant phase. *Polymer* **2010**, *51*, 1450-1456.
(42) Kostromin, S. G.; Sinitzyn, V. V.; Talroze, R. V.; Shibaev, V. P.; Platé, N. A. Thermotropic liquid crystalline polymers, 12. Smectic "C" phase in liquid crystalline polyacrylates with CN-containing mesogenic groups. *Makromol. Chem. Rapid Commun.* **1982**, *3*, 809-814.
(43) Kimura, H.; Nakano, H. Statistical Theory of Surface Tension and Molecular Orientations at the Free Surface in Nematic Liquid Crystals. *J. Phys. Soc. Jpn.* **1985**, *54*, 1730-1736.
(44) Okano, K. Anisotropic Excluded Volume Effect and Alignment of Nematic Liquid Crystal in a Sandwich Cell. *Jpn. J. Appl. Phys.* **1983**, *22*, L343.
(45) Percec, V.; Tomazos, D. Can the rigidity of a side-chain liquid-crystalline polymer backbone influence the mechanism of distortion of its random-coil conformation? *Polymer* **1990**, *31*, 1658-1662.
(46) Ujiie, S.; Kato, T. Design and Synthesis of side chain liquid crystal polymers. In: Goodby, J. W.; Collings, P. J.; Kato, T.; Tschierske, C.; Gleeson, H. F.; Raynes, P. Eds. *Handbook of Liquid Crystals 2nd ed.7*; Willey-VCH, Weinheim, 2014.

Table 1 Contact angle of water droplet on PCBA films

Film thickness / nm	Contact angle θ_w / ° (after annealing)
200	93.6±1.7
140	94.5±0.7
80	91.8±1.6
30	92.1±0.5
15	94.3±1.6
7	91.9±0.4

Scheme and Figure Captions

Scheme 1. Chemical structure of the side chain LC polymer.

Figure 1. White light interference microscopic images of PCBA films of 140 nm (a), 30 nm (b), and 7 nm (c) thickness after annealing at 135 °C for 10 min. The bold line in each image is a scratched region with a spatula to expose the substrate surface. In each part, a height profile is shown.

Figure 2. UV-Vis absorption spectra of PCBA films at 135 °C (red) and 80 °C (blue) with various film thickness of 140 (a), 30 (b), 15 (c), and 7 nm (d). Note that the scale of absorbance axis is altered for each figure.

Figure 3. (a) Absorbance at 300 nm (π–π* band of CB) at 135 °C (isotropic) and 80 °C (smectic A) (a) and absorbance ratio of A_{300}/A_{225} (b) as a function of film thickness of PCBM. Note that the scale of film thickness axis is changed between 60 and 150 nm.

Figure 4. GI-SAXS (Cu $K\alpha$, 0.154 nm) data of PCBA films with 140 (a), 30 (b) and 15 (c) nm thickness at 80 °C, and with 140 nm thickness at 90 °C (d). In each part, upper and lower figures display 2D-XRD patterns and 1D intensity profiles (black: in-plane direction, red: out-of-plane direction), respectively.

Figure 5. 2D GI-SAXS images for 30 nm thick PCBA film using a synchrotron tender X-ray (0.539 nm). Measurements were performed at α_i = 0.41 (Λ = 7 nm) (a), 0.48 (Λ = 11 nm) (b), 0.50 (Λ = 16 nm) (c), 0.56 (Λ = 167 nm) (d), 0.74 (Λ = 453 nm) (e), 0.81 (Λ = 560 nm) (f). Note that α_c (0.54 °) is positioned between (c) and (d).

Figure 6. Schematic representation of CB mesogen orientations in films of varied film thickness, 140 nm (a), 30 nm (b), 10 nm (c), and 7 nm (d). Purple circles denote the cyano group at the terminal of mosogen. Note that the antiparallel interactions are attained among the CB mesogens at thickness above 10 – 15 nm. At 7 nm thickness, such LC structuring is lost.

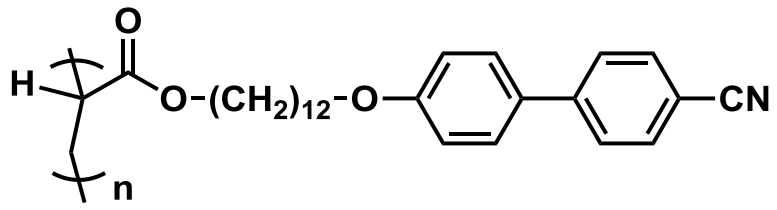

PCBA (n = 28)

Scheme 1

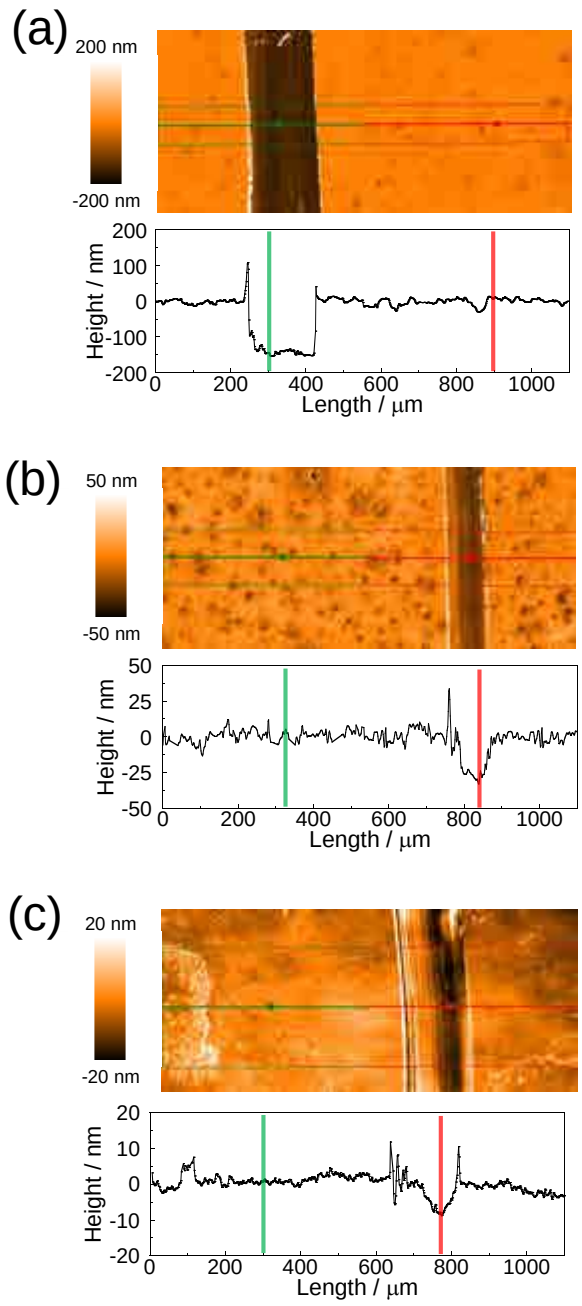
(a)
200 nm
-200 nm
Height / nm
200
100
0
-100
-200
0
200
400
600
800
1000
Length / μm
(b)
50 nm
-50 nm
Height / nm
50
25
0
-25
-50
0
200
400
600
800
1000
Length / μm
(c)
20 nm
-20 nm
Height / nm
20
10
0
-10
-20
0
200
400
600
800
1000
Length / μm

Figure 1

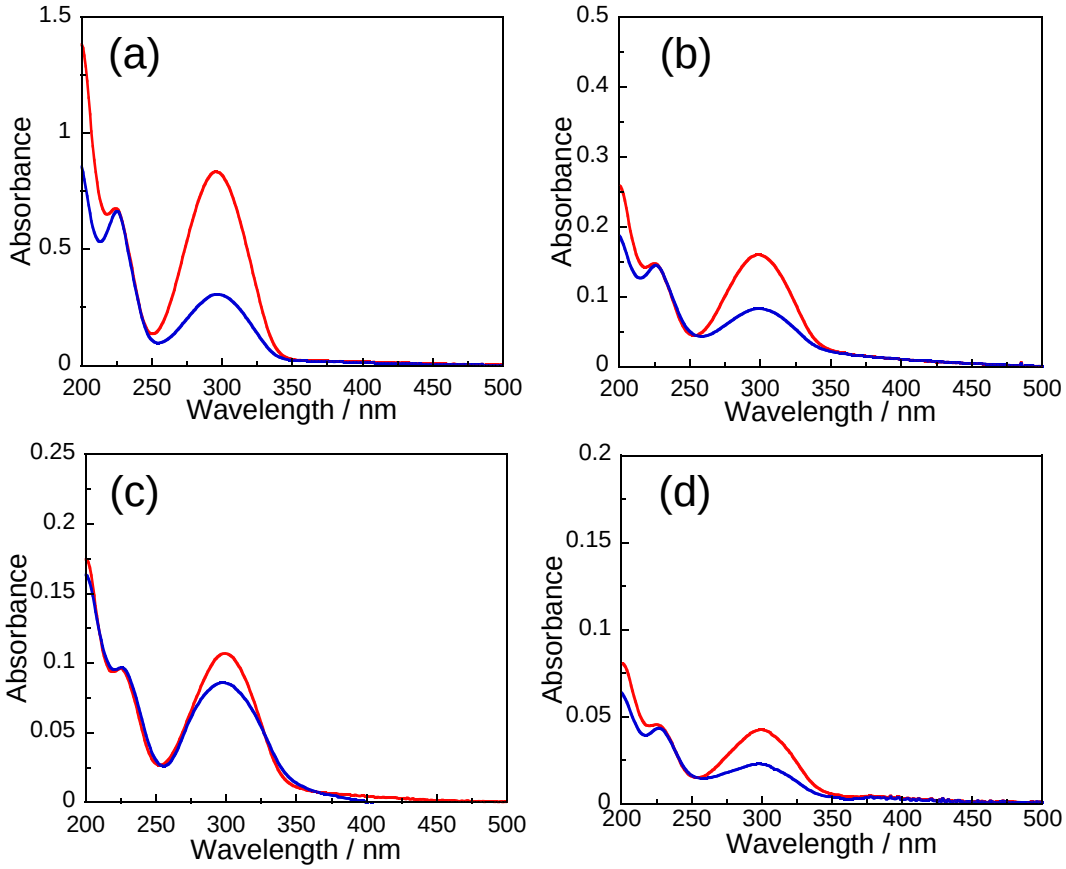

Figure 2

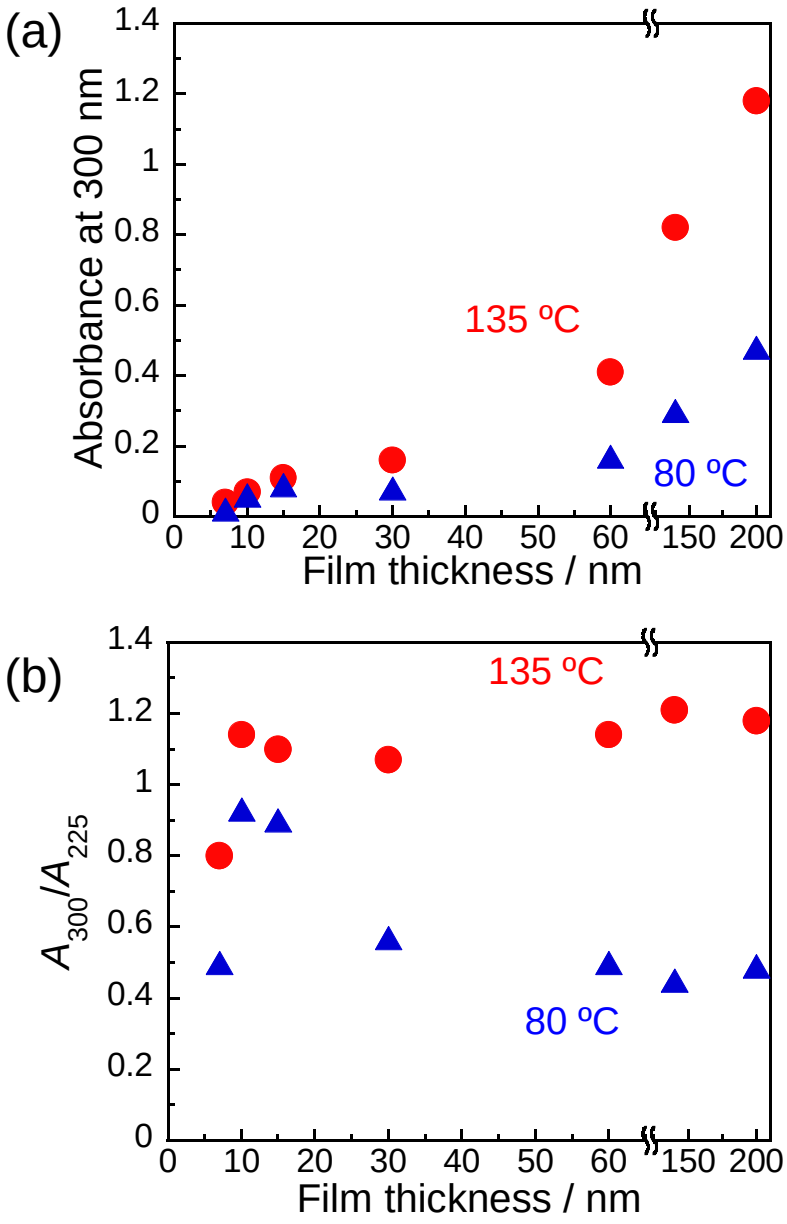
(a)
Absorbance at 300 nm
1.4
1.2
1
0.8
0.6
0.4
0.2
0
135 ºC
80 ºC
0
10
20
30
40
50
60
150
200
Film thickness / nm
(b)
A_{300}/A_{225}
135 ºC
80 ºC
Film thickness / nm

Figure 3

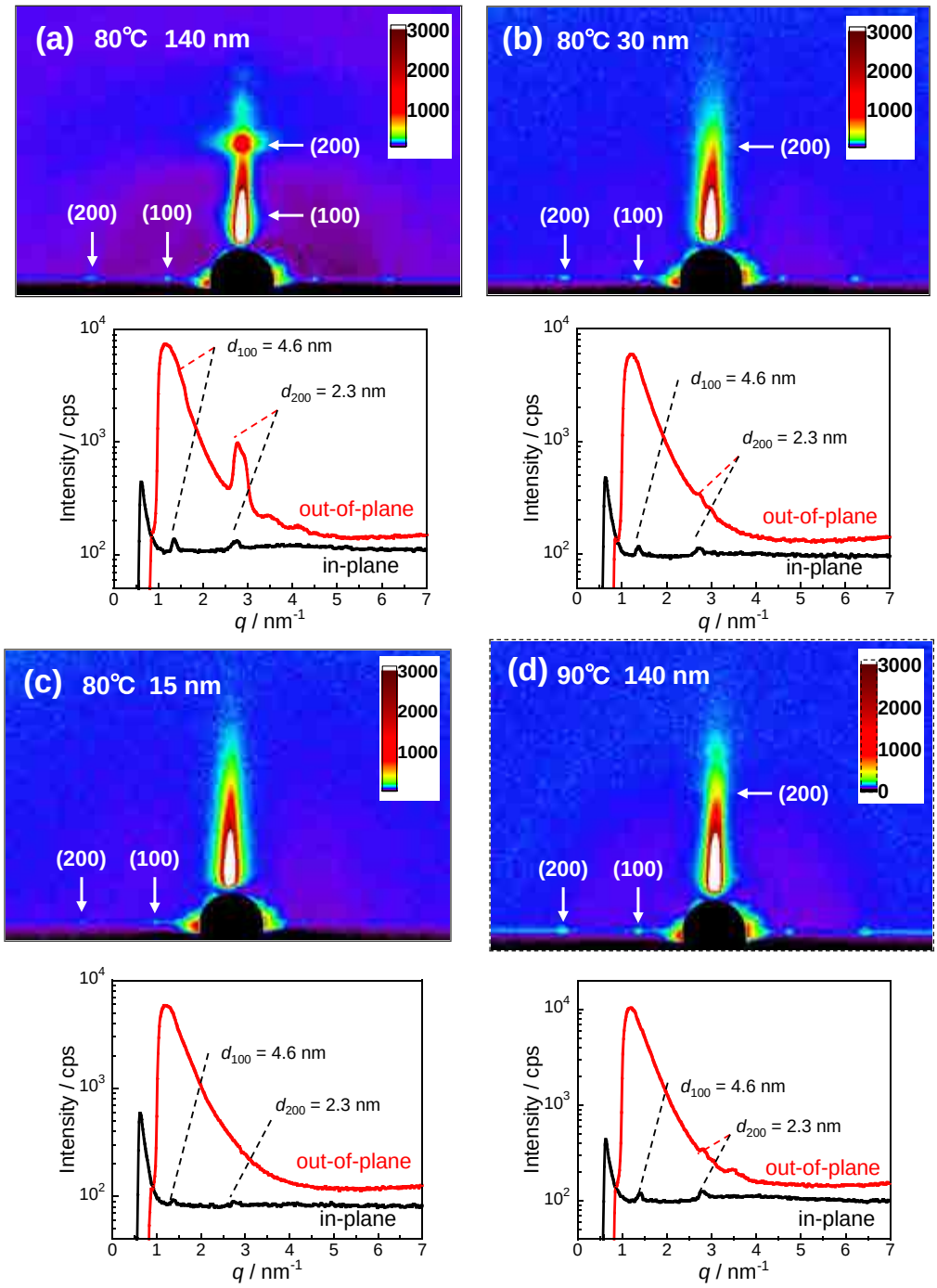
(a) 80℃ 140 nm
3000
2000
1000
(200)
(200)
(100)
(100)
(b) 80℃ 30 nm
3000
2000
1000
(200)
(200)
(100)
d_{100} = 4.6 nm
d_{200} = 2.3 nm
out-of-plane
in-plane
Intensity / cps
q / nm^{-1}
(c) 80℃ 15 nm
3000
2000
1000
(200)
(100)
(d) 90℃ 140 nm
3000
2000
1000
0
(200)
(200)
(100)

Figure 4

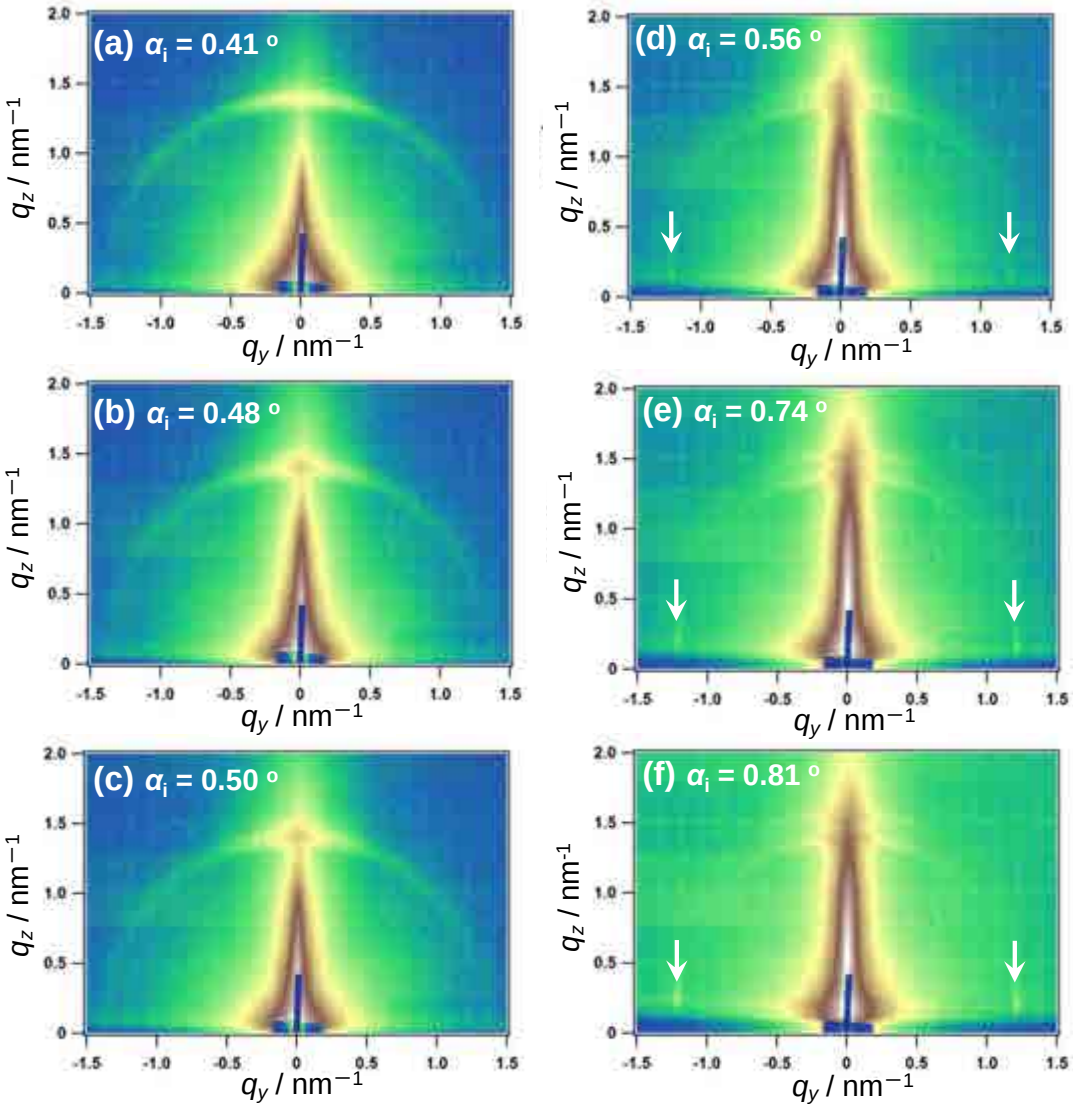
(a) α_i = 0.41 °
(b) α_i = 0.48 °
(c) α_i = 0.50 °
(d) α_i = 0.56 °
(e) α_i = 0.74 °
(f) α_i = 0.81 °
q_z / nm^{-1}
q_y / nm^{-1}

Figure 5

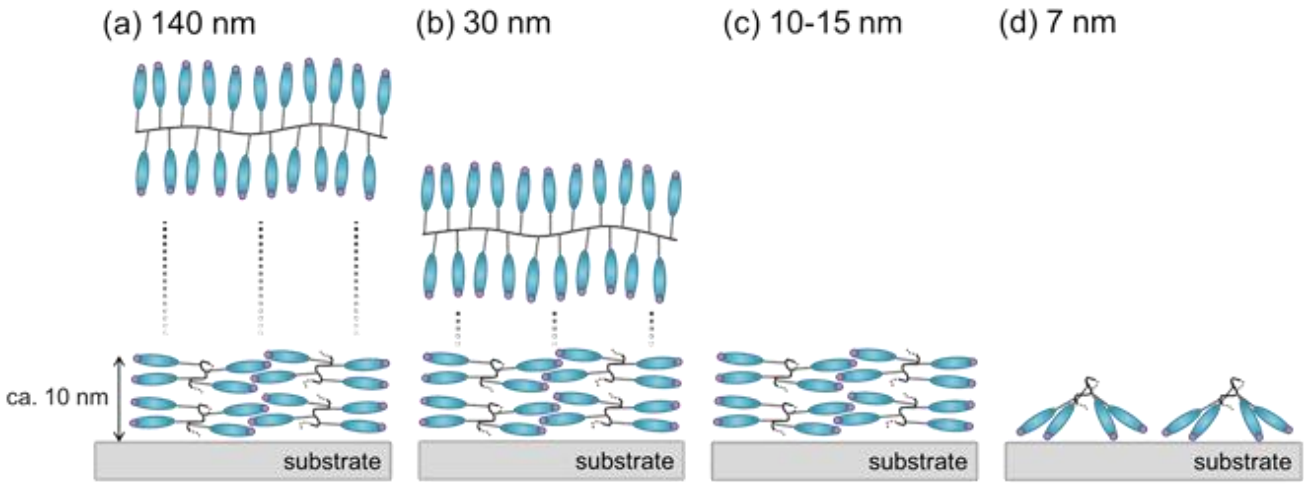
(a) 140 nm
(b) 30 nm
(c) 10-15 nm
(d) 7 nm
ca. 10 nm
substrate
substrate
substrate
substrate

Figure 6

TOC Graphic

Evaluations of Mesogen Orientation in Thin Films of Polyacrylate with Cyanobiphenyl Side Chain

Daisuke Tanaka, Tasuku Mizuno, Mitsuo Hara, Shusaku Nagano, Itsuki Saito, Katsuhiro Yamamoto, and Takahiro Seki**

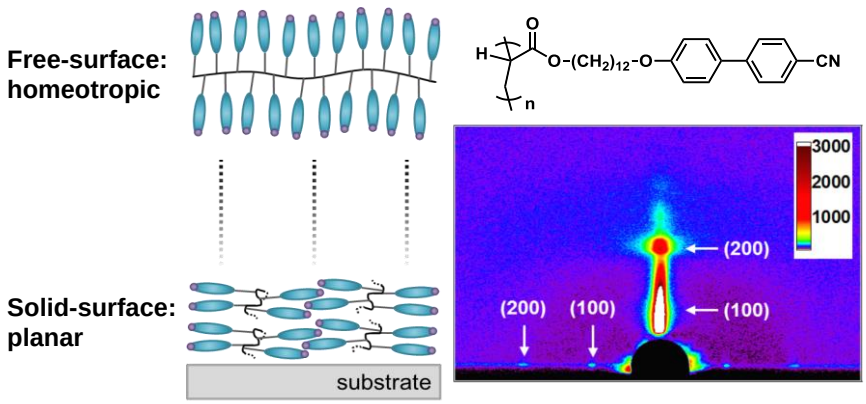

KEYWORDS: side chain liquid crystalline polymers, cyanobiphenyl, mesogen orientation, GI-SAXS